



Geochronology of Massif-Type Anorthosites from the Ubendian Belt, Tanzania

Nelson Boniface

Geology Department, University of Dar es Salaam, P. O. Box 35052, Dar es Salaam, Tanzania

Email address: nelson.boniface@udsm.ac.tz

Received 12 Feb 2020, Revised 27 Apr 2020, Accepted 29 Apr 2020, Published June 2020

DOI: <https://dx.doi.org/10.4314/tjs.v46i2.7>

Abstract

Massif-type anorthosites occur in East Africa at the margins of the Tanzania Craton in the Ubendian Belt. The massif assemblage constitutes of mafic-composition plutons (meta-anorthosite and meta-gabbro), ultramafic plutons, and titaniferous iron-ore. Silicic orthogneisses (tonalitic, dioritic, and granodioritic intrusives) also occur in the vicinity of the said massif-type anorthosites. This article presents ages of meta-anorthosites and meta-gabbros. The new U-Pb zircon age indicates that meta-gabbros and meta-anorthosites crystallized between 1915 ± 24 and 1905 ± 24 Ma concomitantly with the silicic magmatic bodies. Geochronological databases indicate that the period between 1920 and 1850 Ma HP-LT metamorphic interface was formed at subduction zone settings in the Ubendian Belt along with emplacement of arc related voluminous batholiths and volcanic rocks. The subduction tectonics was probably a driving engine for magmatism in the region. A Neoproterozoic metamorphic event dated at 547 ± 25 Ma reworked the Ubendian Belt massifs-type anorthosites.

Keywords: Ubendian Belt, massif-type Anorthosites, U-Pb zircon ages

Introduction

Global Proterozoic massif-type anorthosites and related suite of more silicic plutons occur as composite batholiths, that are temporally restricted to a period between ≈ 2600 and 500 Ma (Ashwal 1993, Arndt 2013, Ashwal and Bybee 2017). Massif-type anorthosites are commonly positioned in linear belts around Archean cratons, where ancient active subduction zones have been identified, e.g. the Grenvillian anorthosites (1050 and 940 Ma) on the outboard continental margins of Laurentia (see Torsvik 2003, Ashwal and Bybee 2017). Thus, Ashwal and Bybee (2017) proposed that Andean-type continental arc setting as

most consistent with the overall observed petrological and structural features in massif-type anorthosites and related rocks. Proterozoic massif-type anorthosites commonly occur with coeval suite of more silicic rocks, but not consanguineous (Ashwal 1993). Similar rock assemblages to the global massif-type anorthosites and associated granitoids occur in Tanzania, in the southern Paleoproterozoic Ubendian Belt (Figure 1).

The Paleoproterozoic Ubendian-Usagaran orogenic Belt binds the southern margins of the Tanzania Craton in East Africa. The Craton and the orogenic belts are separated by a prominent interface of

silicic batholiths (e.g. the Ubena granitoids) and volcanic rocks (e.g. Ngualla and Ndembera volcanics) (Figure 1). Further to the south, at the intersection of the NW trending Ubendian Belt and NE trending Usagaran Belt, intrude the massif-type anorthosite (known as the Upangwa meta-anorthosite complex) along with silicic batholiths and volcanic rocks (Figure 1). Apart from the massif-type anorthosite, the rest of plutonic and volcanic rocks in this

region have received research attention for the last two decades and are known to have been emplaced between 1959.6 ± 1.1 and 1857 ± 19 Ma in a tectonically active continental arc settings (Figure 1, Table 1, Sommer et al. 2005, Fritz et al. 2005, Boniface et al. 2012, Lawley et al. 2014, Many and Maboko 2016, Thomas et al. 2016, Tulibonywa et al. 2015, Bahame et al. 2016, Tulibonywa et al. 2017).

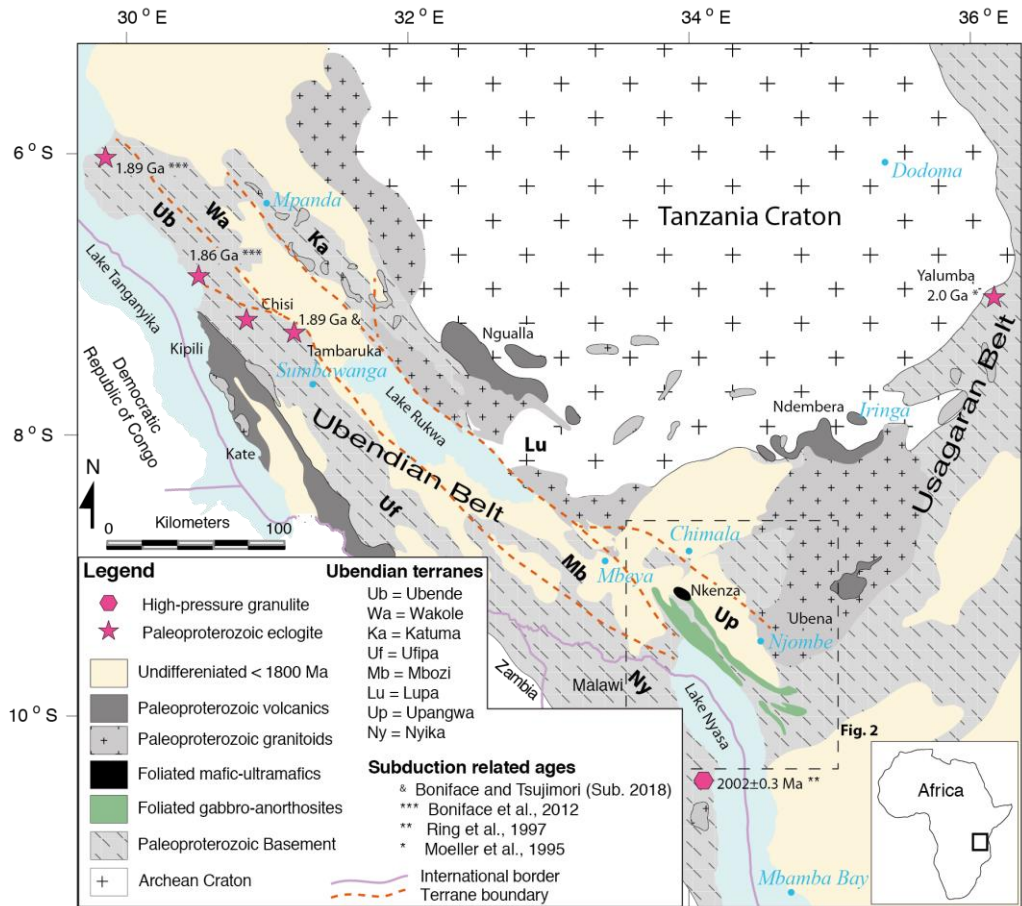


Figure 1: Geological map of the Ubendian-USagaran Belt locating the position of the Upangwa terrane, the Ubendian Belt terrane boundary is according to Daly (1988) and the map was modified after Pinna et al. (2004) and Legler et al. (2015).

Table 1: Compilation of geochronological data from different terranes of the Ubendian Belt

Terrane (Daly 1988)	Magmatic ages	Metamorphic ages	Authors
Ufipa (Gneissic granite)	1864 ± 32 Ma (Granite: U-Pb Zircon) 1864 ± 32 Ma (Granite: U-Pb Zircon)		Lenoir et al. (1994) Lenoir et al. (1994)
		1901 ± 37 – 1949 ± 16 Ma (Grt-By-Ky gneiss: U-Pb Zircon) 1919 ± 12 Ma (Grt-By-Ky gneiss: U-Th-Pb Monazite) 566 ± 6 – 556 ± 5 Ma (Grt-By-Ky gneiss: U-Th-Pb Monazite) 590-520 Ma (Eclogite: U-Pb Zircon)	Boniface and Appel (2018) Boniface and Appel (2018) Boniface and Appel (2018) Boniface and Schenk (2012)
Lupa (Metavolcanics)	1930 ± 3 Ma (Granodiorite: U-Pb Titanite) 1924 ± 13 Ma (Granodiorite: U-Pb Zircon) 1758 ± 33 Ma (Olivine Diabase Dike: U-Pb Zircon) 1878 ± 15 Ma (Granite: U-Pb Zircon) 1875 ± 12 Ma (Porphyritic Dacite: U-Pb Zircon) 1943 ± 32 Ma (Basaltic Andesite: U-Pb Zircon)		Lawley et al. (2014) Manyá (2012) Manyá (2012) Tulibonywa et al. (2015) Tulibonywa et al. (2015) Tulibonywa et al. (2015)
Upangwa (Meta-anorthosite)	2084 ± 86 Ma (Granite: U-Pb Zircon)		Lenoir et al. (1994)
	1797 ± 44 Ma (Gneiss Protolith: U-Pb Zircon)	1045 ± 25 Ma (Gneiss: U-Pb Zircon)	Thomas et al. (2016)
	1880-1850 Ma (Tonalite: U-Pb Zircon)		Manyá and Maboko (2016)
	724 ± 6 Ma (Granite: U-Pb Zircon)		Lenoir et al. (1994)
	842 ± 80 Ma (Granite: U-Pb Zircon)		Lenoir et al. (1994)
		1808 ± 9 Ma (Metapelite: U-Th-Pb Monazite) 944 ± 4 Ma (Metapelite: U-Th-Pb Monazite) 565 ± 4 - 559 ± 8 Ma (Metapelite: U-Th-Pb Monazite)	Boniface and Appel (2017) Boniface and Appel (2017) Boniface and Appel (2017)
	1927 ± 7 Ma (Tonalitic orthogneiss: U-Pb Zircon) 1898 ± 5 Ma (Granitoid orthogneiss: U-Pb Zircon) 1910 ± 6 Ma (Msusule tonalite: U-Pb Zircon) 1909 ± 7 Ma (Igawa orthogneiss: U-Pb Zircon) 1896 ± 6 Ma (Biotite diorite: U-Pb Zircon) 1893 ± 5 Ma (Granodiorite: U-Pb Zircon) 1892 ± 6 Ma (Kangaga porphyritic granite: U-Pb Zircon) 1408 ± 6 Ma (Chimala potassic granite: U-Pb Zircon)		Thomas et al. (2019) Thomas et al. (2019) Thomas et al. (2019) Thomas et al. (2019) Thomas et al. (2019) Thomas et al. (2019) Thomas et al. (2019)
	1915 ± 24 Ma (Meta-gabbro: U-Pb Zircon) 1905 ± 24 Ma (Meta-anorthosite: U-Pb Zircon)		This study This study
	547 ± 25 Ma (Meta-anorthosite: U-Pb Zircon)	This study	
Nyika (Cordierite granulites)		2002 ± 0.3 Ma (Enderbitic gneiss: Pb-Pb Zircon)	Ring et al. (1997)
	1990 - 1930 Ma (Granite: U-Pb Zircon) 1010 ± 22 Ma (Eclogite Protolith: U-Pb Zircon)	1930 ± 30 to 1969 ± 0.4 Ma (Metapelite: Pb-Pb Zircon) 530 - 500 Ma (Eclogite: U-Pb Zircon)	Ring et al. (1997) Ring et al. (2002)

The Upangwa massif-type anorthosites comprise a complex of meta-igneous rock assemblage that range from anorthositic plutons, titaniferous iron-ore bodies, and mafic-ultramafic plutons (e.g. the Nkenza mafic-ultramafic plutons) (Figure 1, Stockley 1948, Haldemann 1961, Evans et al. 2012). The trace element patterns of the Upangwa meta-anorthosites and the associated plutons have affinity to continental arc magmas pointing to their eruption at active continental margins (Evans et al. 2012, Many and Maboko 2016, Boniface 2020). Despite the geologic and economic significance of the Upangwa anorthosites and mafic-ultramafic bodies, there is a gap of geochronological data from this group of rocks. Consequently, petrologic and time relations between the anorthosites and the rest of the Ubendian magmatic and metamorphic bodies have remained unknown. Therefore, the aims of this article were: to establish the ages of the anorthosites and associated gabbros, to determine their chronological relations with the rest of the Ubendian lithological units and fit them in the stratigraphy of Tanzania.

Geological setting

Magmatism: Plutonic and volcanic bodies

The Paleoproterozoic Ubendian and Usagaran Belts are mainly composed of non-foliated and foliated plutonic and volcanic rocks along with highly deformed ortho-gneisses, para-gneisses, and granulites. The magmatic intrusive and extrusive bodies are more prominent at the boundary of the Tanzania Craton where they are given names such as Ubena granitoids, Ndembera metavolcanics, and Ngualla metavolcanics (Figure 1). The Ubendian Belt (Lupa Terrane) is intruded by Ngualla metavolcanics (meta-rhyolite, meta-dacite, meta-andesite, and meta-agglomerate), metabasites (diorite, appinite, and gabbro), and Bt ± Hbl-granites, Hbl-granodiorite, syenogranite, Bt-Ms granite that were emplaced between 1959.6 ± 1.1 and $1919 \pm$

37 Ma (Figure 1, Macfarlane 1965, Lawley et al. 2013, 2014, Tulibonywa et al. 2015, Thomas et al. 2016). The entire package of pluto-volcanic rocks in the Lupa Terranes have strong calc-alkaline magmas affinity and have REE elements with features like magmas that erupt in the continental convergent margins (Lawley et al. 2013, Tulibonywa et al. 2017).

Magmatic bodies along the Usagaran Belt e.g. the calc-alkaline Ndembera metavolcanics with crystallization age between 1921 ± 14 and 1871 ± 15 Ma are coeval with foliated syntectonic granitoids, which intruded along ductile strike-slip shear zones between 1942 ± 89 and 1877 ± 7 Ma probably in the continental arc setting (e.g. Sommer et al. 2005, Fritz et al. 2005, Bahame et al. 2016). The ages of the calc-alkaline Ndembera metavolcanics and the associated foliated syntectonic granitoids overlap with the crystallization ages (1927 ± 7 - 1892 ± 6 Ma) of orthogneisses (tonalitic, dioritic, and granodioritic intrusives) from southern Ubendian Belt around Chimala town (Figure 1, Thomas et al. 2019). Similar but slightly younger crystallization ages between 1887 ± 11 and 1857 ± 19 Ma are documented from non-foliated high-K, I-type granites, and tonalites that crop out around Njombe town in southern Ubendian Belt in the Upangwa Terrane (Figure 1, Many and Maboko 2016).

HP-LT metamorphic interfaces

In Orosirian Period (2050 - 1800 Ma), the Ubendian and Usagaran Belts experienced episodes of subduction related metamorphism (eclogites and high-pressure granulites) at the southern margins of the Tanzania Craton. The Usagaran orogenic cycle recorded the earliest relics of oceanic crust rocks that subducted about 2000 Ma (Yalumba Hill as eclogites) and the subduction event was followed by a collision tectonics about 1999 Ma (Figure 1, Möller et al. 1995, Collins et al. 2004). Whereas, the Ubendian orogenic cycle

records a relatively younger relics of oceanic crust rocks that subducted between 1920 and 1860 Ma (Figure 1, Table 1, Boniface et al. 2012, Boniface and Tsujimori 2014). The Ubendian Belt eclogites crop out in the Ubende and Upangwa Terrane (Figure 1). However, an occasional old metamorphic component dating about 2000 Ma is also recorded by high-pressure granulites and in highly deformed orthogneisses in the Ubendian Belt (Ring et al. 1997, Boniface 2011, Kazimoto et al. 2014).

The Ubendian-Usagaran Belt hosts younger subduction related eclogites with metamorphic ages between 600 and 500 Ma (Ring et al. 2002, Boniface and Schenk 2012). The Neoproterozoic subduction event was a driving force of a metamorphic reworking event that peaked between 570 and 550 Ma and affected the entire Ubendian - Usagaran Belt (Boniface and Appel 2017, 2018, Boniface 2019).

Gabbro-anorthosites plutons

The study area is located at the southern end of the Ubendian Belt where is locally known as the Upangwa Terrane (Daly 1988). The Upangwa Terrane is one of the several lithotectonic terranes of the Ubendian Belt, which is mainly characterized by large masses of metamorphosed mafic igneous rock complex that range from meta-anorthosite to meta-gabbro batholiths sometimes referred to as the Upangwa Meta-Anorthosite Complex. The basic igneous rock complex is accompanied by isolated bodies of ultrabasic plutons (meta-pyroxenite, talcose rocks, serpentinite, dunite, and websterite) and isolated titaniferous magnetite seams (iron ore) (Figure 1, Stockley 1948, Haldemann 1961, Evans et al. 2012). The mafic-ultramafic igneous rocks of the Upangwa Meta-Anorthosite Complex range from non-

foliated (non-metamorphic) to highly metamorphosed rocks reaching up to amphibolite and or granulite facies metamorphic conditions with garnet and migmatitic in places (Haldemann 1961).

Gabbroic and anorthositic batholiths of the southern Ubendian Belt intruded lower crustal rocks (para-gneisses: e.g. biotite gneisses, garnet-biotite-sillimanite gneisses, and orthogneisses: e.g. amphibolites, granulites and felsic gneisses) (Evans et al. 2012, Said and Kamihanda 2015, Boniface and Appel 2017). The orthogneisses (tonalitic, dioritic, and granodioritic intrusives) from around Chimala town have crystallization ages that range between 1927 ± 7 and 1892 ± 6 Ma (Figure 2, Thomas et al. 2019). Whereas, less deformed plutons (high-K, I-type granites, and tonalites) from the same region (around Njombe town) have younger crystallization ages ranging between 1887 ± 11 and 1857 ± 19 Ma (Figure 2, Manya and Maboko 2016). The paragneisses (garnet-biotite-sillimanite gneisses) in the Upangwa Terrane are migmatized and overprinted by three metamorphic and deformation episodes dated at 1808 ± 9 Ma, 944 ± 4 Ma and $565 \pm 4 - 559 \pm 8$ Ma (Boniface and Appel 2017).

In some places, the gabbro - anorthosite complex intrusions of the Upangwa Meta-Anorthosite Complex occur together with lenses of mafic-ultramafic intrusions, which host chromite, platinum, palladium, and gold (e.g. Haldemann 1961, Evans et al. 2012). The mafic - ultramafic lenses, e.g. the Nkenza (in some literature Nkenja) mafic-ultramafic body, comprises several lensoidal tectonic blocks of either mafic (amphibolite) or ultramafic composition (variably serpentinitized dunite and pyroxenite), separated by anastomosing green-schist facies ductile shear zones (e.g. Evans et al. 2012).

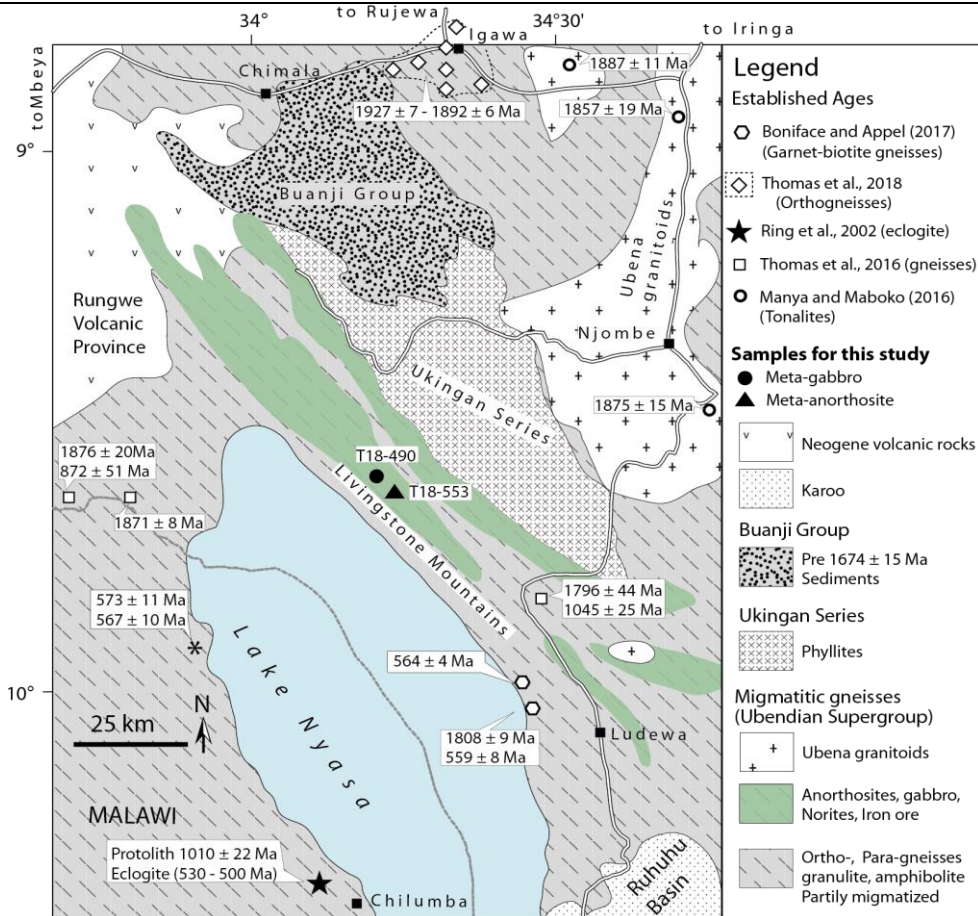


Figure 2: Geological map of the study area illustrating sample locations and field lithological relations, modified from QDS 273 after Said and Kamihanda (2015).

Several petrographic and macroscopic observations led Evans et al. (2012) to conclude that the Nkenza mafic-ultramafic body is probably part of a dismembered ophiolite, and that the body could represent remnants of the original oceanic upper crust (homogenous gabbro and sheeted dykes) of an ophiolite. This conclusion is supported by the composition of amphibolites forming the sheared base of the Nkenza mafic-ultramafic body, which has affinity to mid-oceanic ridge basalt (MORB) or back-arc basalt (BAB) geochemical signatures (Evans et al. 2012).

Materials and Methods

Samples and petrographic description

Meta-anorthosites crop out frequently in the study area along with meta-gabbros and iron-ore bodies. Meta-anorthosites magmatic bodies form isolated hills with diameters at about tenth to hundredth meter scale. Similarly, meta-gabbros and iron-ore bodies crop out on isolated hills in similar dimensions as meta-anorthosite outcrops.

At the outcrop scale, meta-anorthosites are foliated, metamorphosed, and banded. The rock is mainly composed of purely elongated plagioclase mega-crystals or elongate and lensoidal layers (schlieren

structures) of plagioclase and mafic minerals (clinopyroxene, ilmenite, magnetite and garnet) at centimeter to millimeter scale (Figure 3a&b). Clinopyroxene, garnet, and magnetite crystals concentrate in dark metamorphic bands (Figure 3b). The

elongate and lensoidal layers of mafic minerals float in the white background of plagioclase (Figure 3b). The term schlieren refers to discontinuous thin, dark layers that appear and fade out (Barbey 2009 and references therein).

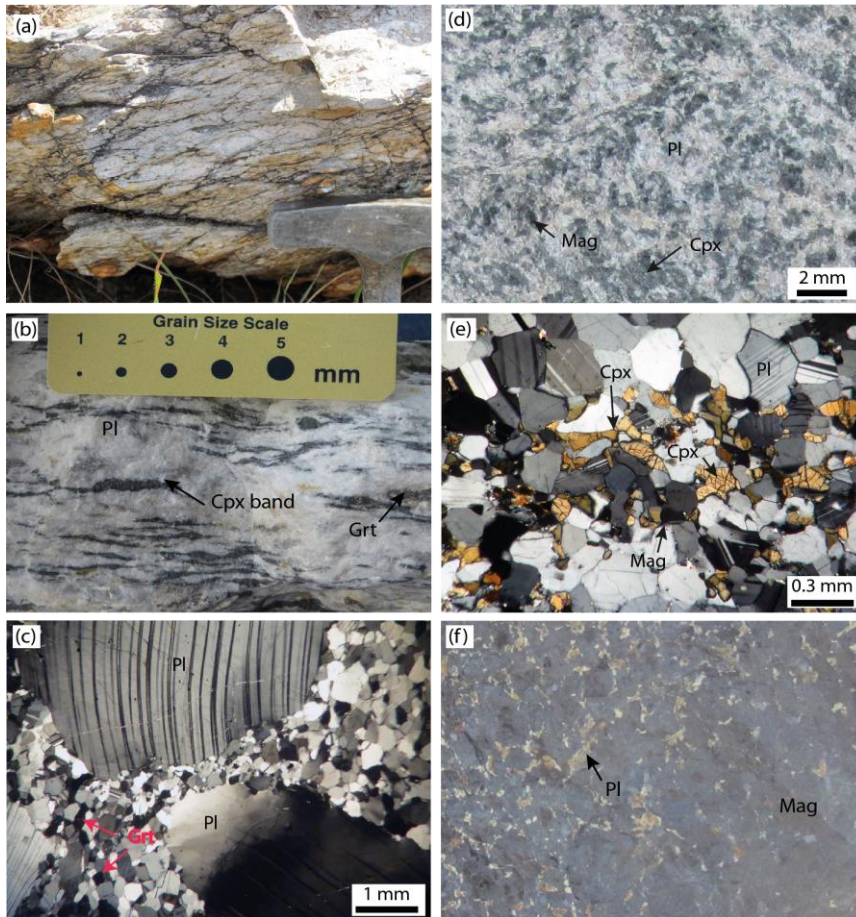


Figure 3: Outcrop, hand specimen, and thin section images of meta-anorthosites, meta-gabbros from southern Ubendian Belt. a) Outcrop of a foliated meta-anorthosite. b) Schlieren structures in meta-anorthosite i.e. elongate and lensoidal concentrations of clinopyroxene, magnetite and garnet. c) Thin section image of a plagioclase porphyroclasts surrounded by recrystallized granoblastic equivalents (the same mineral) in meta-anorthosites. d) Meta-gabbro a weak foliated fabric. e) Thin section image of a weakly foliated meta-gabbro. f) Magnetite rich rock with disseminations of plagioclase.

One fresh meta-anorthosite sample (T18-553) was chosen for petrographic analysis and geochronological studies. Microscopic observations of sample T18-

553 indicated that plagioclase occurs as twinned, stretched, kink-banded porphyroclasts (Figure 3c). The margins of plagioclase porphyroclasts are partly

recrystallized to fine-grained polygonal aggregates of untwined grains of plagioclase. Small grains of garnet and magnetite grow at the margins recrystallized aggregates of plagioclase (Figure 3c).

Meta-gabbros are also foliated; however, the degree of foliation is not as strong as in anorthosites (Figure 3d). Meta-gabbros mainly consist of clinopyroxene and plagioclase and minor amount of magnetite. Plagioclase in meta-gabbros is also kink banded but it is not strongly recrystallized as in anorthosites (Figure 3e). It should also be noted that other units than meta-gabbros and meta-anorthosites with strong metamorphic bands of (dark bands: clinopyroxene, orthopyroxene and garnet, white bands: plagioclase) were identified in the field (see Said and Kamihanda 2015). Rock units which are mainly composed of magnetite (magnetite ore) and disseminations of plagioclase or clinopyroxene also occur in association with gabbroic and anorthositic metamorphosed rock masses (Figure 3f). Most magnetite rich rocks are mainly composed magnetite (> 90%) and other minerals less than 10%.

Analytical techniques

Two rock samples (≈ 7 kg mass per sample, one meta-anorthosite and one meta-gabbro) were taken for zircon separation and handpicking at the African Minerals and Geosciences Centre and the University of Dar es Salaam, Tanzania. Zircon grains were separated from the individual rock samples by conventional mineral separation methods (Holman-Wilfley shaking table, magnetic and heavy liquid separation). Cathodoluminescence (CL) of zircons in 1-inch diameter epoxy-mounts were observed using a SEM Hitachi S-3400N, equipped with a Gatan MiniCL system, in Tohoku University. The CL observation was conducted using a 25 kV accelerating voltage and a 90 nA probe current.

Zircon U-Pb dating was carried out in the Okayama University of Sciences by

using an iCAP-RQ single-collector quadrupole ICP-MS (Thermo Fisher Scientific, Waltham, USA) coupled to an Analyte G2 ArF excimer laser ablation (LA) system equipped with HelEx 2 volume sample chamber (Teledyne Cetac Technologies, Omaha, USA).

The regions of zircon free of metamict part, cracks and inclusion minerals were chosen for the analysis by observing on LA camera unit with reflected and transmitted light. Before the analysis, the analytical spots were pre-ablated using a pulse of the laser with large laser sizes (50 – 85 μm) for removing potential surface contaminant on the zircon surfaces. After laser shooting with laser shutter closed for 30 s (laser warming up), the analytical spots of the zircon were ablated for 30 s by the laser with fluence of 1.7 or 1.8 J/cm², repetition rate of 4 or 5 Hz, and laser spot size diameter of 12 or 15 μm . At the ablation, He gas was introduced into HelEx 2 volume sample chamber (MFC1) and the HelEx arm (MFC2) as a carrier gas. The flow rate into MFC1 and MFC2 was set to 0.5 L/min and 0.3 L/min, respectively. Ablated sample aerosols in He gas were carried through the signal-smoothing device "squid" to the ICP-MS.

The ICP - MS was optimized using continuous ablation of a NIST SRM 612 glass standard to provide maximum sensitivity while maintaining low oxide formation (232 Th/16 O/232 Th < 1%). On the ICP-MS, 6 nuclides (²⁰²Hg, ²⁰⁴Pb, ²⁰⁶Pb, ²⁰⁷Pb, ²³²Th and ²³⁸U) were analyzed. The background and ablation data for each analysis were collected for 15 s of the laser warming-up time and 20 s of the ablation time, respectively. Those data are acquired for multiple groups of 15 unknown grains bracketed by trio of analyses of the 91500 zircon standard (Wiedenbeck et al. 1995, 2004) and NIST SRM612 glass standard, which are corrected for ²⁰⁶Pb/²³⁸U and ²⁰⁷Pb/²⁰⁶Pb ratios, respectively. As normalization value of 91500 zircon

standard, apparent $^{206}\text{Pb}/^{238}\text{U}$ without common Pb correction was used (Sakata et al. 2017, i.e. $206\text{ Pb}/238\text{ U} = 0.17928 \pm 0.00018$). The instrumental mass bias of $^{207}\text{Pb}/^{206}\text{Pb}$ ratios was corrected by normalizing to compiled values of NIST SRM612 glass standard by Jochum et al. (2008).

The background intensities collected at the laser warming-up time were subtracted from following signals at the ablations. The intensity of ^{202}Hg of all analyses was used to correct the isobaric interference of ^{204}Hg on ^{204}Pb . Corrected ^{204}Pb intensities were too low to correct U-Pb ages for common Pb contamination with sufficient precision based on ^{204}Pb (Stern 1997). Thus, in this study, no common Pb correction was made. All uncertainties are quoted at a 2- σ level to which repeatability of each six measurements of 91500 zircon data bracketing unknown sample groups is propagated. Elemental fractionation of U/Pb and Th/U ratios and mass fractionation of

$^{207}\text{Pb}/^{206}\text{Pb}$ ratio were linearly interpolated by the measured data of each six analysis of 91500 zircon and NIST SRM612, respectively. ^{235}U intensities were calculated from ^{238}U using a $^{238}\text{U}/^{235}\text{U}$ ratio of 137.88 (Jaffey et al. 1971). Data presented below were processed using IsoplotR: a free and open toolbox for geochronology of Vermeesch (2018).

Results

Sample T18-553: Meta-anorthosite

The meta-anorthosite sample T18-553 was not rich in zircon. Therefore, only 3 zircon grains, but that gave reasonable age information, were recovered from ≈ 7 kg mass sample. Zircon grains are subrounded and have diameters reaching up to 300 μm . Under light reflecting microscope zircon grains are clear to light brownish. In CL images zircon grains exhibit oscillatory zoned cores which are surrounded by light or dark luminescent rims (Figure 4a).

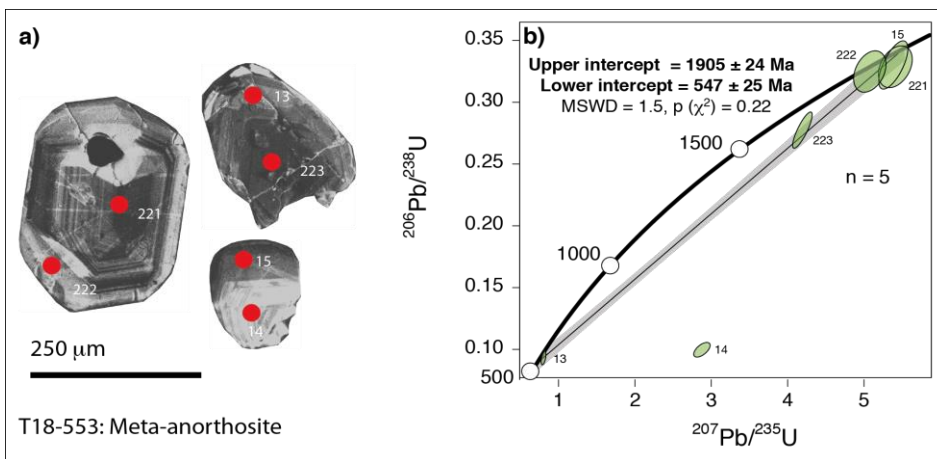


Figure 4: a) CL images of zircon grains from sample T18-553: meta-anorthosite. b) Concordia diagram of the dated meta-anorthosite sample from the Upangwa Terrane.

The analyses show a systematic Pb-loss with variable degree of discordance ($1 - (^{206}\text{Pb}/^{238}\text{U}[\text{age}]/^{207}\text{Pb}/^{206}\text{Pb}[\text{age}]) * 100$) ranging between 2 and 79% and defines an isochron with a lower intercept age at 547 ± 25 Ma and an upper intercept age at $1905 \pm$

24 Ma (Table 2 and Figure 4b). The upper intercept age is interpreted as the crystallization age of the anorthosite protolith and the lower intercept age may relate to metamorphic overprint, which caused Pb-loss in some of the zircons.

T18-490: Meta-gabbro

The meta-gabbro sample has the majority of elongate light-brown zircon grains reaching up to 500 μm long along with some stubby zircons. All the zircon grains have dark CL-response and display no oscillatory zones (Figure 5a).

The analyses show strong Pb-loss with variable degree of discordance (1-

$(^{206}\text{Pb}/^{238}\text{U} [\text{age}]/^{207}\text{Pb}/^{206}\text{Pb} [\text{age}]) * 100$) ranging between 16 to 87 % and defines an isochron with a lower intercept age at 206 ± 9 Ma and an upper intercept age at 1915 ± 24 Ma (Table 2 and Figure 5b). The upper intercept age is interpreted as the crystallization age of the gabbro protolith and the lower intercept age may relate to a younger tectonic disturbance, which caused Pb-loss in the zircons.

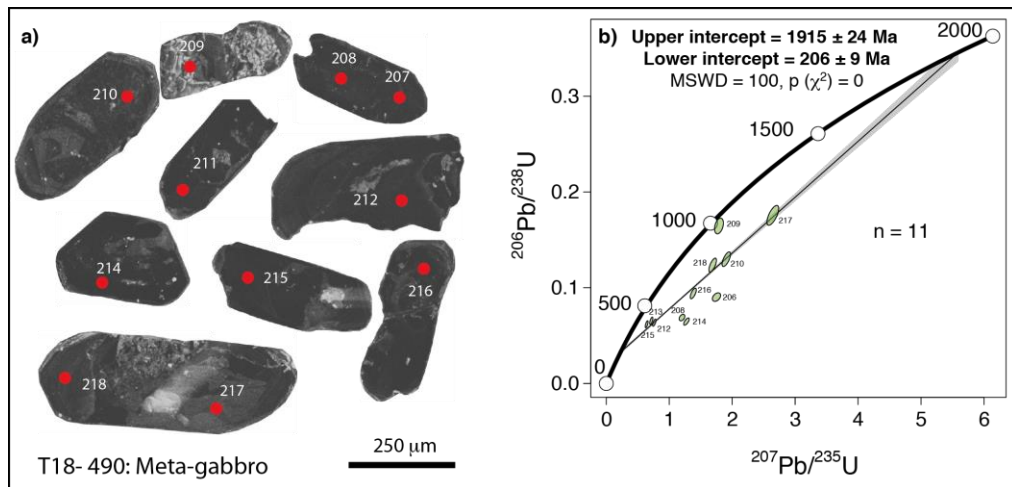


Figure 5: a) CL images of zircon grains from sample T18-490: Meta-gabbro. b) Concordia diagram of the dated meta-gabbro sample from the Upangwa Terrane.

Interpretation and discussion

Paleoproterozoic magmatism

The U-Pb zircon age data obtained in this study provide a time window during when the massif-type anorthosites from southern Ubendian Belt crystallized. The crystallization age of the meta-anorthosite body at 1905 ± 24 Ma is concomitant with the crystallization age of the associated gabbro at 1915 ± 24 Ma. These new geochronological data are hereby interpreted as the emplacement age of the meta-anorthosites, meta-gabbros, iron-ore, and mafic-ultramafic rock assemblage of the Upangwa Meta-Anorthosite Complex at the intersection of the Usagaran and Ubendian Belt. Evans et al. (2012) observed that the lower section of the Nkenza mafic-

ultramafic body (considered to be part of the Upangwa Meta-Anorthosite Complex) has affinity to mid-oceanic ridge basalt (MORB) or back-arc basalt (BAB) geochemical signatures. Therefore, they concluded that the Nkenza mafic-ultramafic body was probably part of a dismembered ophiolite, and that the body could represent remnants of an original oceanic upper crust of an ophiolite. Thus, the new U-Pb zircon age data obtained from this study probably provide the timing of convergent continental margins that existed between 1915 ± 24 and 1905 ± 24 Ma in southern Ubendian Belt where it intersects with the Usagaran Belt.

Table 2: U-Pb zircon geochronological data a meta-gabbro (sample T18- 490) and a meta-anorthosite (sample T18- 490). All errors are at the 2 σ confidence level

	$^{238}\text{U}/$ ^{206}Pb	Error	$^{207}\text{Pb}/$ ^{206}Pb	Error	$^{238}\text{U}/^{206}\text{Pb}$ and $^{207}\text{Pb}/^{206}\text{Pb}$ Error correlation	$^{207}\text{Pb}/$ ^{235}U Age [Ma]	Error	$^{206}\text{Pb}/$ ^{238}U Age [Ma]	Error	$^{207}\text{Pb}/$ ^{206}Pb Age [Ma]	Error	$^{207}\text{Pb}/^{235}\text{U}-$ $^{206}\text{Pb}/^{238}\text{U}$ Age [Ma]	Error	%Disc
T18-490: Meta-gabbro														
206	11.085	0.2260	0.141	0.0028	0.7117	1027.34	9.94	556.8	10.9	2236.2	34.8	720.4	11.1	75
207	17.114	0.3494	0.203	0.0041	0.7104	982.86	9.74	366.09	7.27	2847.6	32.9	373.36	7.81	87
208	14.530	0.2964	0.127	0.0026	0.7104	801.8	8.57	429.06	8.47	2053.2	35.7	543.64	8.5	79
209	6.079	0.1243	0.079	0.0017	0.6987	1041.8	10.5	981.7	18.6	1170.1	41.5	1034	10.4	16
210	7.705	0.1866	0.107	0.0019	0.8043	1083.26	9.64	786.7	17.9	1740.7	32.8	1121.78	9.76	55
211	15.552	0.3769	0.077	0.0014	0.7991	529.92	6.03	401.73	9.44	1128.6	36.3	531.38	6.28	64
212	15.745	0.3813	0.087	0.0016	0.8032	575.68	6.37	396.96	9.32	1363	34.6	568.36	6.89	71
213	15.264	0.3698	0.079	0.0014	0.8003	547.54	6.17	409.06	9.6	1175.2	35.9	549.1	6.45	65
214	15.467	0.3745	0.143	0.0025	0.8067	834	8.2	403.87	9.48	2262.3	30.6	504.4	12.8	82
215	16.160	0.3914	0.075	0.0014	0.8016	502.91	5.77	387.06	9.1	1071.8	36.3	506.41	5.96	64
216	10.636	0.2575	0.107	0.0019	0.8058	881.23	8.51	579.3	13.4	1742.1	32.6	890	9.42	67
217	5.694	0.1379	0.109	0.0020	0.8047	1313.2	10.7	1042.9	23.3	1786.6	32.6	1359.9	10.1	42
218	8.087	0.1959	0.099	0.0018	0.8043	1004.77	9.24	751.6	17.2	1607.7	33.3	1037.9	9.3	53
T18-553: Meta-anorthosite														
13	10.748	0.2619	0.063	0.0013	0.7575	599.25	7.29	573.5	13.4	698	44.7	598.81	7.33	18
14	10.031	0.2457	0.209	0.0041	0.7803	1376.1	11.6	612.6	14.3	2900.6	31.8	583.2	20.2	79
15	3.029	0.0734	0.118	0.0021	0.8039	1882.2	12.4	1839.2	38.8	1929.9	32.1	1889.5	11.1	5
221	3.042	0.0641	0.119	0.0026	0.6948	1886.4	14.4	1832.3	33.6	1946.6	39	1884.4	14.4	6
222	3.078	0.0650	0.113	0.0025	0.6898	1832	14.5	1813.6	33.4	1853.1	40	1831.2	14.4	2
223	3.604	0.0780	0.110	0.0014	0.8556	1672.7	10.2	1578.8	30.3	1792.7	23.8	1701.58	7.3	12

The southern Ubendian Belt is also intruded by ortho-gneisses (tonalitic, dioritic, and granodioritic intrusives), which crystallized between 1921 ± 14 and 1871 ± 15 Ma (Thomas et al. 2019). These data clearly indicate that the silicic ortho-gneisses and the meta-anorthosites of southern Ubendian Belt have strikingly similar emplacement ages. The association of silicic intrusives and massif-type anorthosite is a common feature of the convergent margins related Proterozoic massif-type anorthosites observed elsewhere in the world (Ashwal 1993). Geochemical features of non-foliated high-K, I-type granites, and tonalites from the same region indicate that convergent continental margins in southern Ubendian Belt continued to exist until about 1887 ± 11 - 1857 ± 19 Ma (Manya and Maboko 2016).

The timing of convergent plate tectonics and emplacement of massif-type anorthosites in the Upangwa Terrane coincide with the period of formation of HP-LT metamorphic interface in the Ubende and Ufipa Terranes of the Ubendian Belt. The ages of HP-LT metamorphic interface between 1920 and 1860 Ma mark a period of formation of eclogites that were derived from subducted oceanic plate (Boniface et al. 2012, Boniface and Tsujimori 2014). The major magmatic events (emplacement of plutonic and volcanic rocks) in the Ubendian - Usagaran Belt cluster between 1920 and 1860 Ma (Sommer et al. 2005, Boniface et al. 2012, Manya and Maboko 2016, Thomas et al. 2016, Tulibonywa et al. 2015, Bahame et al. 2016, Tulibonywa et al. 2017, Thomas et al. 2019). The Ubendian Belt subduction event was probably the driving force of magmatic bodies emplacement in Ubendian - Usagaran Belt.

Neoproterozoic reworking

The Neoproterozoic age at 547 ± 25 Ma obtained from a meta-anorthosite sample dates a period of metamorphic reworking in the region. This age conforms to the

geochronological data from previous publications (Ring et al. 2002, Boniface and Schenk 2012, Boniface and Appel 2017, 2018, Thomas et al. 2019, Boniface 2019). The accumulation of geochronological data from these different authors indicate that many parts of the Ubendian - Usagaran Belt were re-worked during the Neoproterozoic Ufipa Orogeny between 600 and 500 Ma, which is coeval with the Kuungan Orogeny in southern Africa (see Fritz et al. 2013, Boniface 2019).

Conclusions

The intersection of the Ubendian and Usagaran Belts hosts metamorphosed massif-type anorthosites associated with silicic magmatic bodies (tonalitic, dioritic, and granodioritic intrusives). Massif-type anorthosites crystallized between 1915 ± 24 and 1905 ± 24 Ma concomitantly with silicic magmatic bodies. The emplacement age of the anorthosites and gabbros of southern Ubendian Belt fall in the time window when voluminous batholiths and volcanic rocks got emplaced at the margins of the Tanzania Craton. A Neoproterozoic metamorphic event dated at 547 ± 25 Ma reworked the Ubendian Belt massifs-type anorthosites.

Acknowledgments

I acknowledge the support of the Geological Survey of Tanzania for thin section preparation and logistical support. Geochronological data were acquired by Tatsuki Tsujimori of the University of Tohoku in Japan and his colleagues from the Okayama University of Sciences in Japan. Other persons who assisted my research at different stages include Abdul Mruma, Msechu Maruvuko, Khalid Musa Nyoka, Godson Kamihanda and Hamisi Saidi.

References

- Arndt N 2013 The formation of massif anorthosite: Petrology in reverse. *Geosci. Front.* 4: 195-198.
- Ashwal LD 1993 Anorthosites. *Springer-*

- Verlag, Berlin pp 422.
- Ashwal LD, Bybee GM 2017 Crustal evolution and temporality of anorthosites. *Earth-Sci. Rev.* 173: 307-330.
- Bahame G, Many S and Maboko MA 2016 Age and geochemistry of coeval felsic volcanism and plutonism in the Palaeoproterozoic Ndembera Group of southwestern Tanzania: Constraints from SHRIMP U-Pb zircon and Sm-Nd data. *Precamb. Res.* 272: 115 - 132.
- Barbey P 2009 Layering and schlieren in granitoids: A record of interactions between magma emplacement, crystallization and deformation in growing plutons. *Geol. Belgica* 12 (3 - 4): 109-133.
- Boniface N 2020 Geochemical characterization of the Paleoproterozoic Massif-Type Anorthosites from the Ubendian Belt, Tanzania. *Tanz. J. Sci.* 46(1): 61-75.
- Boniface N 2011 Petrography and geochemistry of mafic granulites of the Ubendian belt: Contribution to insights into the lower continental crust of the Paleoproterozoic. *Tanz. J. Sci.* 37: 129-143.
- Boniface N 2019 An overview of the Ediacaran-Cambrian orogenic events at the southern margins of the Tanzania Craton: Implication for the final assembly of Gondwana. *J. Afr. Earth Sci.* 150: 123-130.
- Boniface N and Appel P 2017 Stenian - Tonian and Ediacaran metamorphic imprints in the southern Paleoproterozoic Ubendian Belt, Tanzania: Constraints from in situ monazite ages. *J. Afr. Earth Sci.* 133: 25-35.
- Boniface N and Appel P 2018 Neoproterozoic reworking of the Ubendian Belt crust: Implication for an orogenic cycle between the Tanzania Craton and Bangweulu Block during the assembly of Gondwana. *Precamb. Res.* 305: 358-385.
- Boniface N and Schenk V 2012 Neoproterozoic eclogites in the Paleoproterozoic Ubendian Belt of Tanzania: Evidence for a Pan- African suture between the Bangweulu Block and the Tanzania Craton. *Precamb. Res.* 208-211: 72-89.
- Boniface N, Schenk V and Appel P 2012 Paleoproterozoic eclogites of MORB-type chemistry and three Proterozoic orogenic cycles in the Ubendian belt (Tanzania): Evidence from monazite and zircon geochronology, and geochemistry. *Precamb. Res.* 192-195:16-33.
- Boniface N and Tsujimori T 2014 Dating of Proterozoic orogenic events around the Tanzania Craton: new insights from in-situ zircon and monazite geochronology. In: IMA2014 (Abstract). Johannesburg, South Africa, p. 204.
- Collins AS, Reddy SM, Buchan C and Mruma A 2004 Temporal constraints on Palaeoproterozoic eclogite formation and exhumation (Usagaran Orogen, Tanzania). *Earth Planet. Sci. Lett.* 224(1-2): 175-192.
- Daly MC 1988 Crustal shear zones in Central Africa: a kinematic approach to Proterozoic tectonics. *Episodes* 11(1): 5-11.
- Evans DM, Barrett FM, Prichard HM and Fisher PC 2012 Platinum-palladium-gold mineralization in the Nkenja mafic-ultramafic body, Ubendian metamorphic belt, Tanzania. *Miner. Deposita* 47: 175-196.
- Fritz H, Abdelsalam M, Ali K, Bingen B, Collins A, Fowler A, Ghebreab W, Hauzenberger C, Johnson P, Kusky T, Macey P, Muhongo S, Stern R and Viola G 2013 Orogen styles in the East African Orogen: A review of the Neoproterozoic to Cambrian tectonic evolution. *J. Afr. Earth Sci.* 86: 65-106.
- Fritz H, Tenczer V, Hauzenberger CA,

- Wallbrecher E, Hoinkes G, Muhongo S and Mogessie A 2005 Central Tanzanian tectonic map: A step forward to decipher Proterozoic structural events in the East African Orogen. *Tectonics* 24 (6), n/a-n/a, tC6013.
- Haldemann EG 1961 Geological map of Milo: QDS 274. Geological map, *Geol. Survey Dept. Dodoma*.
- Jaffey AH, Flynn KF, Glendenin LE, Bentley WC and Essling AM 1971 Precision measurement of half-lives and specific activities of ²³⁵U and ²³⁸U: a review. *Phys. Rev. C* 4: 1889-1906.
- Jochum KP, Brueckner SM, Nohl U, Stoll B and Weis U 2008 Geostandards and geoanalytical research bibliographic review 2007. *Geostand. Geoanal. Res.* 32(4): 509-514.
- Kazimoto EO, Schenk V and Berndt J 2014 Neoproterozoic and Paleoproterozoic crust formation in the Ubendian Belt of Tanzania: Insights from zircon geochronology and geochemistry. *Precambrian Res.* 252: 119-144.
- Lawley C, Selby D, Condon D and Imber J 2014 Palaeoproterozoic orogenic gold style mineralization at the Southwestern Archaean Tanzanian cratonic margin, Lupa Goldfield, SW Tanzania: Implications from U-Pb titanite geochronology. *Gondwana Res.* 26(3-4): 1141-1158.
- Lawley CJ, Selby D, Condon DJ, Horstwood M, Millar I, Crowley Q and Imber J 2013 Litho-geochemistry, geochronology and geodynamic setting of the Lupa Terrane, Tanzania: Implications for the extent of the Archaean Tanzanian Craton. *Precamb. Res.* 231: 174-193.
- Legler C, Barth A, Knobloch A, Mruma AH, Myumbilwa Y, Magigita M, Msechu M, Ngole T, Stanek KP, Boniface N, Kagya M, Manya S, Berndt T, Stahl M, Gebremichael M, Dickmayer E, Repper C, Falk D and Stephan T 2015 Minerogenic Map of Tanzania and Explanatory Notes for the Minerogenic Map of Tanzania 1:1.5 M. Geol. Survey of Tanzania.
- Lenoir JL, Liégeois JP, Theunissen K and Klerkx J 1994 The Palaeoproterozoic Ubendian shear belt in Tanzania: geochronology and structure. *J. Afr. Earth Sci.* 19 (3): 169-184.
- Macfarlane A 1965 Geological map of Gwa: QDS 208. Geological map, *Geol. Survey Tanzania*.
- Manya S and Maboko MA 2016 Generation of Palaeoproterozoic tonalites and associated high-K granites in southwestern Tanzania by partial melting of underplated mafic crust in an intracontinental setting: Constraints from geochemical and isotopic data. *Lithos* 260: 120-133.
- Möller A, Appel P, Mezger K and Schenk V 1995 Evidence for a 2 Ga subduction zone: eclogites in the Usagaran belt of Tanzania. *Geology* 23(12): 1067-1070.
- Pinna P, Muhongo S, Mcharo BA, Le Goff E, Deschamps Y, Ralay F and Milesi JP 2004 Geology and mineral map of Tanzania at 1:2,000,000.
- Ring U, Kröner A and Toulkeridis T 1997 Palaeoproterozoic granulite-facies metamorphism and granitoid intrusions in the Ubendian-Usagaran Orogen of northern Malawi, east-central Africa. *Precamb. Res.* 85(1-2): 27-51.
- Ring U, Kröner A, Buchwaldt R, Toulkeridis T and Layer PW 2002 Shear-zone patterns and eclogite-facies metamorphism in the Mozambique belt of northern Malawi, east-central Africa: implications for the assembly of Gondwana. *Precamb. Res.* 116(1-2): 19-56.
- Said H and Kamihanda G 2015 Explanatory notes of the geology of Lupula: QDS 273 - Geology. Explanatory notes, Geol. Survey of Tanzania.
- Sakata S, Hirakawa S, Iwano H, Danhara T, Guillong M and Hirata T 2017 A new approach for constraining the

- magnitude of initial disequilibrium in Quaternary zircons by coupled uranium and thorium decay series dating. *Quatern. Geochronol.* 38: 1-12.
- Sommer H, Kröner A, Muhongo S and Hauenberger C 2005 SHRIMP zircon ages for post-Usagaran granitoid and rhyolitic rocks from the Palaeoproterozoic terrane of southwestern Tanzania. *S. Afr. J. Geol.* 108: 247-256.
- Stern R 1997 The GSC Sensitive High Resolution Ion Microprobe (SHRIMP): Analytical techniques of zircon U-Th-Pb age determinations and performance evaluation. In: Th-eriault RJ. (Ed.), Radiogenic age and isotopic studies: Report 10. *Geol. Survey Canada*, pp. 1-31.
- Stockley GM 1948 Geology of north, west and central Njombe district, southern highlands province. Bulletin 18, *Geol. Survey Tanganyika*.
- Thomas RJ, Jacobs J, Elburg MA, Mruma A, Kamihanda G, Kankila A, Masanja A and Saidi H 2019 New U-Pb-Hf zircon isotope data for the Paleoproterozoic Ubendian belt in the Chimala area, SW Tanzania. *Geosci. Front.* 10(6): 1993-2006.
- Thomas RJ, Spencer C, Bushi AM, Baglow N, Boniface N, de Kock G, Horstwood MS, Hollick L, Jacobs J, Kajara S, Kamihanda G, Key RM, Maganga Z, Mbawala F, McCourt W, Momburi P, Moses F, Mruma A, Myambilwa Y, Roberts NM, Saidi H, Nyanda P, Nyoka K and Millar I 2016 Geochronology of the central Tanzania Craton and its southern and eastern orogenic margins. *Precamb. Res.* 277: 47-67.
- Torsvik TH 2003 The Rodinia jigsaw puzzle. *Science* 300: 1379-1381.
- Tulibonywa T, Many S and Maboko MA 2015 Palaeoproterozoic volcanism and granitic magmatism in the Ngualla area of the Ubendian Belt, SW Tanzania: Constraints from SHRIMP U-Pb zircon ages, and Sm-Nd isotope systematics. *Precamb. Res.* 256: 120-130.
- Tulibonywa T, Many S, Torssander P and Maboko MA 2017 Geochemistry of the Palaeoproterozoic volcanic and associated potassic granitic rocks of the Ngualla area of the Ubendian Belt, SW Tanzania. *J. Afr. Earth Sci.* 129: 291-306.
- Vermeesch P 2018 IsoplotR: A free and open toolbox for geochronology. *Geosci. Front.* 9(5): 1479-1493.
- Wiedenbeck M, All-e P, Corfu F, Griffin W, Meier M, Oberli F, Quadt AV, Roddick J and Spiegel W 1995 Three natural zircon standards for U-Th-Pb, Lu-Hf, trace element and REE analyses. *Geostand. Newslet.* 19(1): 1-23.
- Wiedenbeck M, Hanchar JM, Peck WH, Sylvester P, Valley J, Whitehouse M, Kronz A, Morishita Y, Nasdala L, Fiebig J, Franchi I, Girard JP, Greenwood R, Hinton R, Kita N, Mason P, Norman M, Ogasawara M, Piccoli P, Rhede D, Satoh H, Schulz-Dobrick B, Skr O, Spicuzza M, Terada K, Tindle A, Togashi S, Vennemann T, Xie Q and Zheng YF 2004 Further characterisation of the 91500 zircon crystal. *Geostand. Geoanal. Res.* 28(1): 9-39.